

RESIDUAL PM and AM NOISE MEASUREMENTS, NOISE FIGURE and JITTER CALCULATIONS of 100 GHz AMPLIFIERS¹

D. A. HOWE* and J. R. OSTRICK**

* National Institute of Standards & Technology, Boulder, CO, USA

** Northrop Grumman Space Technology (NGST), Redondo Beach, CA, USA

Abstract

We report the first definitive PM and AM noise measurements at 100 GHz of indium phosphide (InP) amplifiers operating at 5 K, 77 K, and room temperature. Amplifier gain ranged from +7 dB to +30 dB, depending on input RF power levels and operating bias current and gate voltages. The measurement system, calibration procedure, and amplifier configuration are described along with strategies for reducing the measurement system noise floor in order to accurately make these measurements. We compute amplifier noise figure with an ideal oscillator signal applied and, based on the PM noise measurements, obtain $NF = 0.8$ dB, or a noise temperature of 59 K. Measurement uncertainty is estimated at ± 0.3 dB. Results show that the use of the amplifier with an ideal 100 GHz reference oscillator would set a lower limit on rms clock jitter of 44.2 fs in a 20 ps sampling interval, if the power into the amplifier were -31.6 dBm. For comparison, clock jitter is 16 fs with a commercial room-temperature amplifier operating in saturation with an input power of -6.4 dBm.

I. INTRODUCTION

100 GHz is a convenient reference (or clock) frequency for emerging digital signal-processing applications. As a result, NIST's Time and Frequency Metrology Group has engaged in a program designed to characterize the components that play critical roles in various applications. For example, reference-oscillator noise sets a basic limit on many system performance criteria including jitter, bit-error-rate, sensitivity, resolution, and dynamic range of these high-speed digital and signal-processing systems [1]. While some work has been done in predicting the PM and AM noise of oscillators, there are few relevant data on the residual noise introduced by one key component, the amplifier. At frequencies below 40 GHz, there are various suitable characterization techniques [2-4], while at W-band frequencies (75 – 110 GHz), characterization techniques are often inconsistent, subject to inaccuracies, or invalid due to high measurement noise [5,6]. These amplifiers are needed not only to deliver reference clock signals, but they are also a necessary component in very wideband communications systems, measurements of the temperature and constituents of the atmosphere, surveillance radars, and both ground-based and spaceborne radio astronomy. Additionally, superconducting electronics based on Josephson junction circuits operating at the 100 GHz range intrinsically have low power and will require amplification with low jitter in order to utilize the low phase noise characteristics of the Josephson junction. Amplifiers cooled to cryogenic temperatures have provided a method to achieve desired sensitivities [7] and match well with the requirements of superconducting electronics.

We report measurements of the PM and AM noise of various W-band amplifiers at room temperature, and the first measurements on an InP amplifier arranged to operate at 77 K and 5 K [7]. In addition, this paper discusses strategies for making state-of-the-art noise measurements at W-band [8]. Section II defines the rationale for using the so-called dual-channel cross-correlation measurement technique. Section III describes the apparatus, including a calibrated AM/PM modulator.

¹ Work of the US Government, not subject to copyright. Sponsorship provided by the Office of Naval Research.

For completeness, commercial products are mentioned in this report. No endorsement is implied. Products are available from other manufacturers.

Sections IV, V, and VI explain how PM and AM cross-correlation measurements are made using the apparatus. Section VII presents PM and AM noise measurements, and section VIII shows the computation of noise figure of the cooled 100 GHz InP amplifier based on measurements described in Section VII. Section IX computes the consequent jitter performance.

II. MOTIVATION FOR DUAL-CHANNEL CROSS-CORRELATION MEASUREMENTS

This writing assumes that the reader has some familiarity with the subject of PM and AM noise measurements on an otherwise ideal oscillating signal. For AM noise measurements, AM level is typically measured using a circuit that rectifies an oscillating carrier signal and produces the absolute value of the signal, essentially converting AC to DC. This rectified output is filtered to separate AM noise modulation from the normal carrier and other high-order signals [2,3].

The most straightforward measurement of PM noise is made by analyzing residual phase fluctuations through the amplifier under test relative to its input phase using a phase discriminator. By having the output and input signals at relative phase quadrature, phase fluctuations through the amplifier will appear as voltage fluctuations out of the mixer, and these voltage fluctuations can be analyzed by a conventional spectrum analyzer [9-12]. More complicated arrangements using heterodyne schemes that down-convert phase fluctuations in intermediate stages can provide marginal improvements, but these measurement schemes can be noisier and more difficult to calibrate and characterize.

An inherent assumption in the typical phase-noise-measurement process is that the noise of the reference oscillator and the components used in the phase detection, particularly the mixer and perhaps an amplifier, are significantly lower than the noise introduced by the amplifier under test. This assumption breaks down in the case of precise measurements of low-temperature, low-phase-noise devices, especially at W-band where measurement-system noise exceeds that of the device under test (DUT). For example at W-band, the $1/f$ (or “flicker”) noise in a phase-noise detector’s mixer, amplifier (if one is necessary), and any isolators will often be greater than the noise in the amplifiers to be tested, particularly if the amplifier is operating at very low temperature. If a harmonic mixer must be used, there is an additional problem of high conversion loss in the up-conversion to W-band, as well as the introduction of spurious signals. Even getting up to and maintaining desirable signal levels of over +10 dBm for mixer inputs can be a problem in the measurement system because of the simple matter of high waveguide attenuation due to hookup tolerances and mechanical distortions (waveguide size is usually WR-10). Due to all these factors, it is desirable to use the dual-channel or the so-called cross-correlation technique [13] for making these noise measurements.

III. MEASUREMENT TEST SET

Our approach to PM and AM noise measurements is based on existing state-of-the-art, cross-correlation noise measurement techniques. The measurement system can switch between two phase-noise and two amplitude-noise detectors whose outputs are analyzed with a cross-correlation spectrum analyzer as previously mentioned. The approach, widely regarded as the best measurement approach at lower frequencies, has some new problems in the W-band frequency range. For example, a new W-band PM/AM modulator had to be constructed to calibrate or normalize the raw measurements. Furthermore, an important factor of concern for W-band is compactness. While X-band systems can be built with a great deal of flexibility to accommodate a variety of component form factors and dimensional changes thanks to the use of coaxial cables, W-band systems do not have the same flexibility. Using WR-10 waveguide components, long or contorted signal paths become detrimental to phase matching and attenuate signals significantly. Furthermore, some specialized components that are needed at W-band are awkward and bulky, especially for making connections to a cryogenic system. Consequently, the hardware of the system’s two channels of phase and amplitude detection has obvious physical considerations. The left side of figure 1 shows a

photograph of the arrangement of the AM/PM noise measurement system, and the right side shows the waveguide hookup to the dewar which contains the InP amplifier.

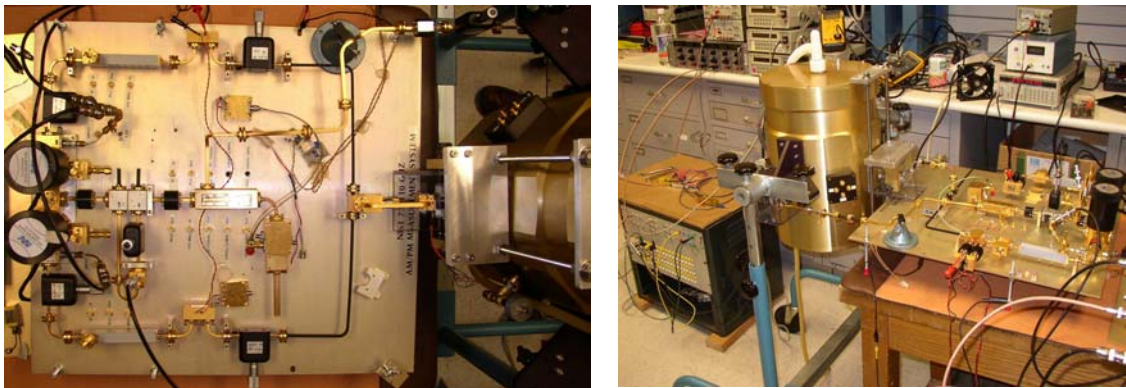


Figure 1: In the left photo, the dual-channel W-band measurement system is shown. The schematic is shown in figure 2. In the right photo, one sees the connection to the cooled amplifier under test inside the dewar. Low-noise battery supplies and meters are shown in the background.

IV. CROSS-CORRELATION PM NOISE MEASUREMENT

The measurement of PM noise at 100 GHz is made by two nearly identical phase bridges whose phase deviations are analyzed simultaneously using a cross-spectrum analyzer. The phase bridges are shown in figure 2 with channel 1 above and channel 2 below.

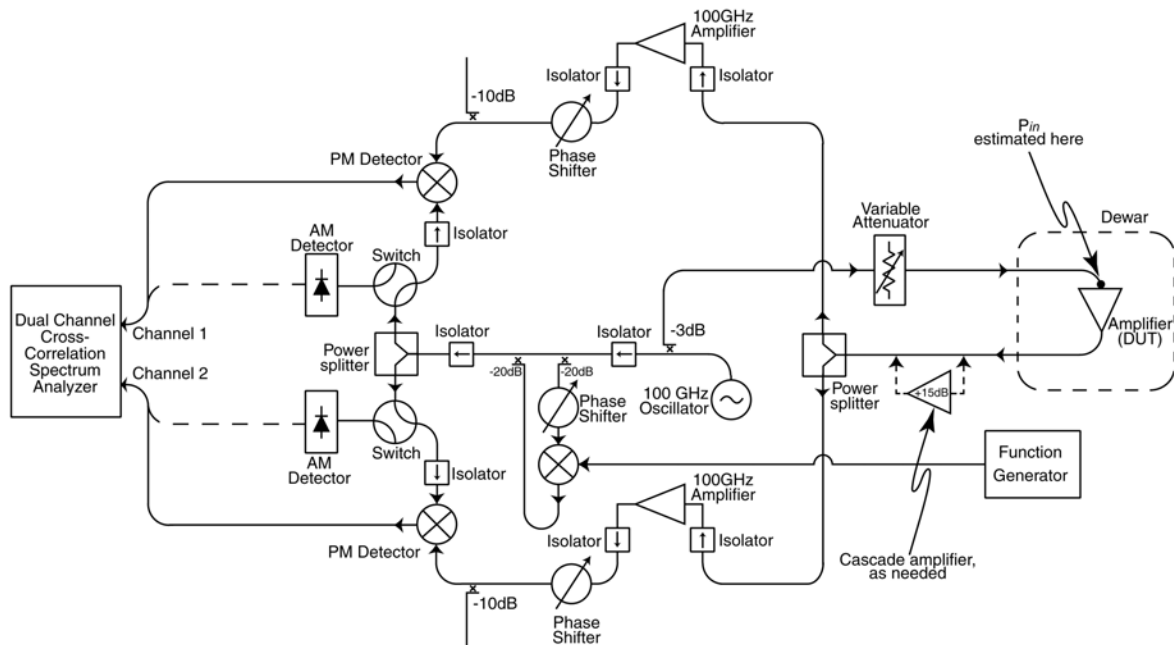


Figure 2: The residual PM noise of an amplifier (DUT) is measured with the configuration shown. Mixer, isolator, and measurement-system amplifier noise in the top PM detectors are uncorrelated with respect to the bottom detectors. The PM noise of the 100 GHz oscillator signal is suppressed, since it appears equally at both inputs to the mixers. Cascade amplifier helps overcome mixer noise.

In this technique, the voltage fluctuations out of the mixers of two separate phase bridges operating at 100 GHz are fed to the two inputs of a dual-channel dynamic signal analyzer. Each channel computes $S_{1,2}(f) = \text{FT } V_{DUT OSC}(t) \cdot \text{FT } V_{REF OSC}(t)$, where FT is a Fourier Transform operator. Thus, in the cross-correlation output between the two channels, only the FT $V_{DUT OSC}(t)$ is observed because the uncorrelated terms due to the measurement system components approaches zero as $1/\sqrt{(2m)}$, where m is an average of the number of complete blocks of data that undergo Fourier transforms, down to the limit of the uncertainty on the uncorrelated noise. In order to make measurements with a low enough measurement-system noise floor and with a modest accuracy goal of ± 1 dB, use of the cross-correlation method and of an accurate calibration procedure are essential. The correlated spectrum, here being the PM noise of a device under test such as an amplifier, is extracted; uncorrelated noise from components in each bridge averages down, thus lowering the measurement system's noise floor and enhancing the precision of the estimate of PM noise.

As discussed, a pair of phase-sensitive detectors operate simultaneously. One input to the pair is the amplifier plus source oscillator, and the other input to the pair is just the source oscillator. In practice, a high degree of mechanical symmetry must exist between the phase bridges, one above and one below as shown. By laying out components so that the delays in each channel are identical, correlated noise plus signals are closely matched in phase at each bridge's mixer (PM detectors). By adjusting the delay from each signal source, for example, when one source includes an amplifier or other DUT, then the PM noise of the 100 GHz driving reference source (a 100 GHz cavity-stabilized Gunn diode oscillator) cancels to a high degree. Both of these factors are important in exploiting the benefits of the cross-correlation technique to ultimately measure the noise, $L(f)$, introduced by the amplifier as if driven by a perfect "noiseless" 100 GHz reference oscillator.

We installed two 90-105 GHz amplifiers with gains of +10 dB to increase the input sensitivity of the cross-correlation measurement system. Their additive noises are uncorrelated and so will effectively decrease the measurement system noise floor with the increase of sensitivity by about the same +10 dB. As will be seen later, these amplifiers are essential for amplifier noise measurements, especially for measurements of a DUT operating at low temperatures.

We also found that signal isolators were needed in several places to reduce correlated noise between the mixers. One wouldn't imagine that isolators would be needed in so many lines because the mixers are driven from a common oscillator, but we found that correlated noise in the mixers actually dominates the suppressed noise of the oscillator (suppressed because its noise appears equally at both mixer ports as discussed above).

V. CROSS-CORRELATION AM NOISE MEASUREMENT

By feeding the signal under test into two AM detectors that are operating in parallel, one obtains two voltages $V_1(t)$ and $V_2(t)$ whose rms values are proportional to AM level for a data run t in seconds. Each detector has intrinsic noise that is uncorrelated relative to the other detector. We extract a measurement of the cross-power spectral-density feature of a two-channel dynamic signal analyzer in order that uncorrelated noise is averaged down as discussed earlier.

Figure 3 shows a diagram of the arrangement for the parallel AM detectors. We note that the AM noise floor is determined by the residual AM noise of the 100 GHz source oscillator. Measurement of the device's PM noise differs from that of the device's AM noise in that the PM noise of the source oscillator cancels to a high degree. There is no way to suppress the AM noise of the 100 GHz reference oscillator in this measurement system; however, we find that the AM noise of the reference oscillator is substantially below the AM noise of the amplifiers under test.

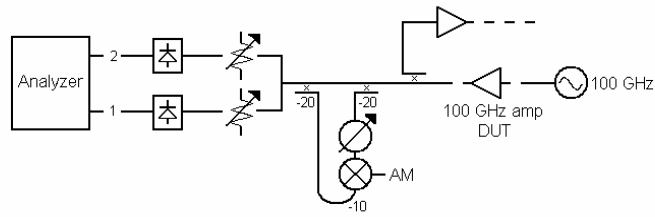


Figure 3: Parallel AM detectors are connected to each channel of a cross-correlation analyzer. The configuration shown in figure 2 is altered to conform to this arrangement for measurement of AM amplifier noise.

VI. PM & AM MODULATOR

A key requirement for high-accuracy noise measurements is to calibrate the dual measurement channels *in situ* using precise PM and AM modulation. Figure 4 shows a diagram and picture of the modulator used to calibrate the sensitivity of the PM and AM measurement test set. While this modulator has been described and successfully used at lower frequencies [12], a key challenge here has been to translate the technique to a modulator at 100 GHz. The important property of this modulator is that it introduces pure PM or AM modulation into the measurement system at a variety of offset Fourier frequencies and at a known level [14]. Cross-guide directional couplers are used for compactness, along with isolators at both the input and output.

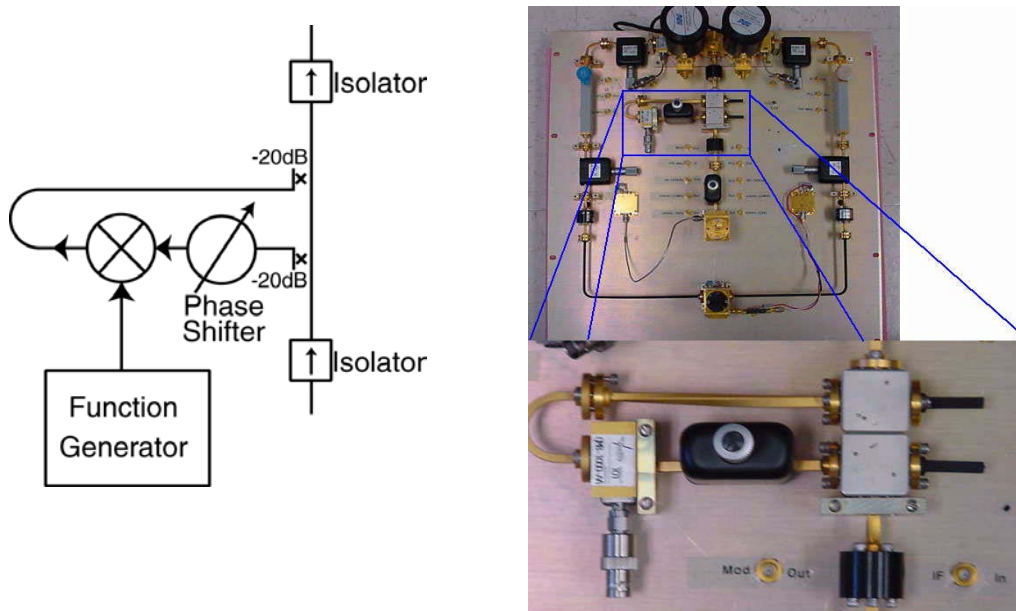


Figure 4: The modulator introduces a fixed level of pure PM or AM modulation for measurement system calibration over the range of frequencies swept by the function generator. The mixer is operated in saturation.

VII. PM & AM NOISE MEASUREMENTS OF 100 GHZ AMPLIFIER

Two 100 GHz, InP amplifiers with MMICs developed by NGST and packaged by the Jet Propulsion Laboratory [7] have been measured using the 100 GHz noise measurement system. One of the amplifiers was mounted in a cryogenic system, illustrated in figure 1, with input and output waveguides penetrating the walls of the dewar. The input stainless steel waveguide has an attenuation of 4.5 dB, while the output Au-plated stainless steel waveguide has an attenuation of

0.6 dB. The cryogenic amplifier has a Millitech WBI Series wide-band isolator in front of it, and all measurements of the cryogenic amplifier considered the amplifier and isolator as a single unit. The amplifier, other than the cryogenic amplifier shall be referred as the RT (room temperature amplifier). Figure 5 shows the amplifier output RF power and gain depending on input RF power for both the cryogenic and RT amplifier has been shown.

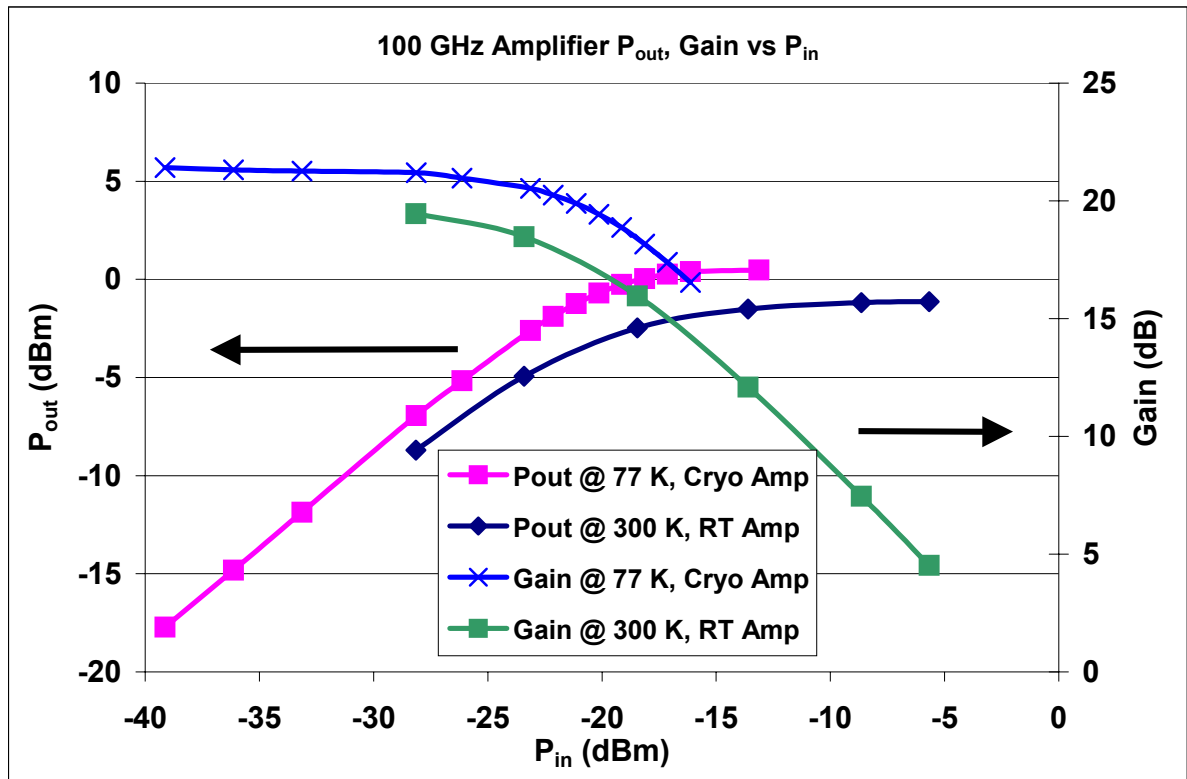


Figure 5: The output RF power and gain of the two 100 GHz InP amplifiers. The cryogenic amplifier cooled to 77 Kelvin has both gates biased at -0.223 V and drain biased at 1.55 V @ 25.2 mA. The RT amplifier at 300 Kelvin has both gates biased at -0.240 V and drain biased at 1.00 V @ 33.9 mA.

Figure 6 shows the PM and AM noise measurements of the 100 GHz InP amplifiers and the noise floor measurements of the NIST 100 GHz measurement system. A flicker PM (f^{-1}) slope is shown at the bottom for reference. Ignoring the "Flicker PM Slope" line, the lower three plots are, in descending order, (1) PM noise floor with the amplifier removed and replaced by a waveguide connection, (2) AM noise of the RT amplifier, and (3) the amplifier-removed AM measurement noise floor. In all cases, the AM noise was significantly below the PM noise of the amplifiers. It exhibited a $1/f$ dependence, achieving a white AM noise level of -155 dBc/Hz at a corner frequency of 100 kHz.

Ground loops were eliminated by floating battery supplies and by using a single-point ground near the amplifier. Battery supply wires were over 1 m long, and stray electromagnetic noise picked up was significant. Even with considerable noise bypassing at the amplifier, we believe the limit of the AM noise performance is related to supply-voltage pickup and not the amplifier itself.

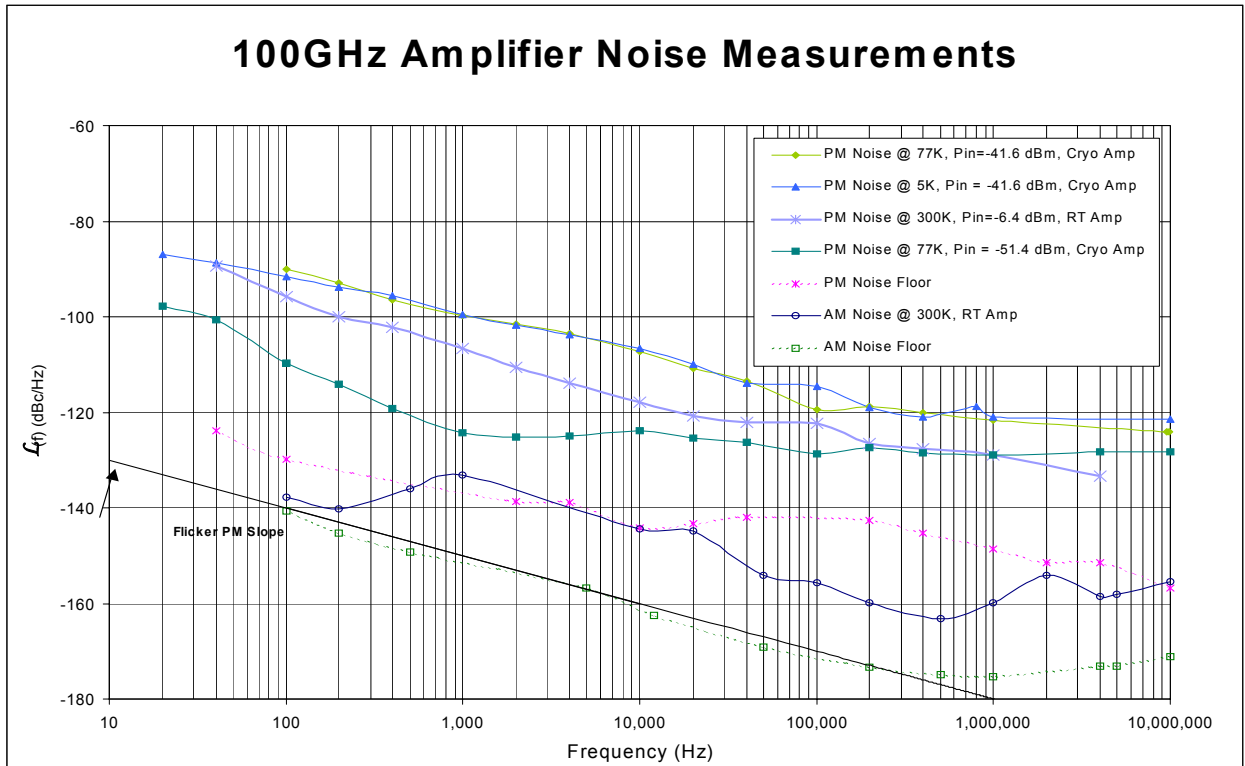


Figure 6: The top four plots are the measured PM noise of the InP amplifiers at various input powers and temperatures. Note that the predominant noise type is flicker PM except for the lowest input power case of $P_{in} = -51.4$ dBm where the broadband white PM noise is readily measurable. The averages of these white PM values were used to compute noise figure. The fifth plot down is the system PM noise floor. The AM noise and noise floor are respectively indicated by the two bottom plots. The gaps are regions where pickup of spectral lines occurred. Flicker PM (f^{-1}) slope is shown at the bottom for reference.

On the other hand, the PM noise is significantly higher and does not have the same AM profile. Stray signal pickup was low enough in measurements of PM noise that we believe the noise shown in figure 6 is inherent to the amplifier under test. The f^{-1} slope indicates a flicker PM (denoted as FLPM) noise type. Close to the carrier (at Fourier frequencies from f equals 1 Hz to 10's of kHz), the noise from amplifiers is not "flat" (that is, not white) but is characterized by flicker noise behavior, which typically follows a f^{-1} dependence. Basically, the inherent near-DC noise of the amplifiers, which is always flicker noise, will be up-converted and projected onto the pure carrier signal being amplified.

For example, the RT amplifier showed the characteristic FLPM noise dependence. The RT amplifier had an input power of -6.4 dBm, which places the amplifier in full saturation. There were no regions of f^0 , or white PM (WHPM) noise, which will be discussed later, while white AM noise was observed from 0.1 MHz to 10 MHz.

In the cooled measurements, we found that within the measurement uncertainty, the noise measurements on the 100 GHz amplifier at 5 K were not substantially different from results at 77 K, meaning within measurement repeatability. Consequently, most tests were done at the more

convenient temperature of 77 K. Measurements at 5 K were used to verify that there was no substantial change in the measurements reported here.

The PM noise of the amplifier used in our low-temperature tests showed a dramatic dependence on the amplifier's input power. In figure 6, one sees that at low input power (-51.4 dBm), the PM noise corresponds to f^{-2} from 20 Hz to 1 kHz and reaches broadband WHPM (f^0) above 1 kHz frequency offset. As the input power increases nearly 10 dB (from -51.4 dBm to -41.6 dBm), the PM noise changes to a flicker PM with a f^{-1} behavior. Consequently, the white PM noise level is reached at a corner frequency which increases from 1 kHz to 10 MHz for only a 10 dB increase in the amplifier's input power (from -51.4 dBm to -41.4 dBm). This indicates substantial amplifier nonlinearity in gain (distortion), and probably accounts for why WHPM noise was not observed in the RT amplifier. With the input power being so high ($P_{in} = -6.4$ dBm), flicker PM noise predominated everywhere below $f = 10$ MHz, which is the high-frequency limit of our dual-channel analyzer.

For two of the PM noise measurements on the cryogenic amplifier, a Quinstar QPN-1A10SZ medium power amplifier with a gain of 15 dB at room temperature was cascaded with the cryogenic amplifier to increase the signal level and overcome the noise of the measurement-system mixers. Since the cryogenic amplifier had high gain, the noise contribution from the second-stage Quinstar amplifier was minimal. At 77 K, with an input power level of -41.6 dBm, the PM noise level of the cryogenic amplifier was measured with and without the Quinstar amplifier in cascade. These two measurements were not significantly different. The second plot from the top of figure 6 represents their average.

The cryogenic amplifier, with an input power level of -51.4 dBm at 77 K, represents a separate PM noise measurement with the Quinstar amplifier in cascade. At this low input power, the use of a second-stage medium power amplifier in this PM measurements is essential to the measurement of the PM broadband white-noise levels of the input amplifier contained in the dewar.

VIII. NOISE FIGURE CALCULATION

While “noise figure” (NF) is a common amplifier specification, it is meaningful only at offset frequencies where phase noise is white; sometimes this means at frequencies more than 10% above and below the carrier frequency itself. In these frequency regions, Josephson junction-based oscillators (JJOs) theoretically expect to have low phase noise [15,16]. Since the JJOs is intrinsically low power technology, the noise figure may be utilized to determine the necessary JJO power level while maintaining the low phase noise of the JJO. A central point is that, in the presence of signals, the noise level, and hence noise figure, is no longer constant (this is indicative of a white noise). In fact, the noise level increases as f decreases as shown in figure 6. This increase is at a rate of at least $1/f$, the “flicker” behavior previously mentioned, which often dominates significantly over the white noise level given by the noise figure measured in the absence of an actual signal through the amplifier. Furthermore, the flicker noise level depends on the amplifier's linearity and input power. Because of this signal-induced rise in amplifier noise, many systems can be seriously compromised, and not achieve performance which is predicted from the no-signal noise figure.

As mentioned earlier, the inherent near-DC noise of an amplifier, which is always flicker noise, is up-converted and projected onto the signal being amplified [17-21]. This amplifier behavior significantly limits the performance of low-noise, spectrally pure oscillators designed as reference clocks for rf and digital systems. Consequently, amplifier merit is often better characterized by a PM noise measurements than by noise figure measurements.

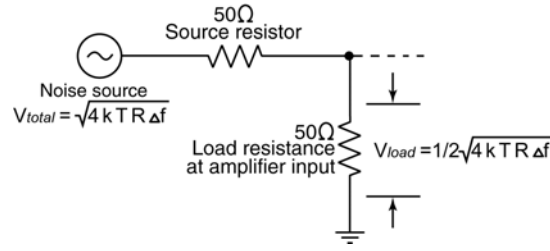


Figure 7: Equivalent input circuit showing the thermal noise generator with a source resistance of 50Ω and terminated into the amplifier's input (load) resistance, which is also 50Ω . Note that the thermal noise voltage is divided in half at the amplifier's input.

We will now compute NF based on PM measurements in the previous section. To derive the formula for such a computation, we start from the definition of the RF power spectrum of an oscillator's signal. For the moment, it is convenient to express this in terms of voltage rather than power so as to avoid the need for carrying the value of the load resistance (50Ω). This is changed in the final formula. The phase noise part of the RF spectrum does not entail a "power" measurement in any case, and the introduction of R for determining thermal noise level becomes less confusing. We can write

$$S_{RF}(f) = \frac{PSDV_N(v_0 - f) + PSDV_N(v_0 + f)}{V_0^2},$$

where V_0 is the rms voltage level of the carrier, $PSDV_N(v_0 \pm f) \equiv V_N^2(v_0 \pm f)$ is the power spectral density of the voltage noise at frequency $v_0 \pm f$, v_0 is the carrier frequency, and f is the offset or Fourier frequency. Since the random RF noise is distributed equally between amplitude and phase modulation noise (equally AM and PM noise), the PSD of just the PM noise, denoted as $S(f)$ in units of rad^2/Hz is half of $S_{RF}(f)$. Using the definition $L(f)_{rad} \equiv \frac{1}{2} S(f)$ [3,4], one obtains

$$L(f)_{rad} = \frac{PSDV_N(v_0 - f) + PSDV_N(v_0 + f)}{(4)V_0^2}.$$

Referring to figure 7, the expected voltage noise V_n of the oscillator's source resistance of 50Ω is $\sqrt{4kTR\Delta f}$, where Boltzmann's constant $k = 1.38 \times 10^{-23}$ J/K, T is in degrees K, R is resistance in Ω , and Δf is the bandwidth. The voltage noise appearing across the load resistance at the input of the amplifier under test is half of this source noise, or $\sqrt{kTR\Delta f}$, as shown in figure 7. With $\Delta f = 1$ Hz, the voltage noise is \sqrt{kTR} . Thus, $V_N^2 = kTR$ can be regarded as the power spectral density $PSDV_n(f)$. Substituting kTR into the expression for $L(f)$ above gives

$$L(f)_{rad} = \frac{(2)kTR}{(4)V_0^2}.$$

$L(f)_{rad}$ expressed in units of dBc/Hz is obtained here by computing $10\log \cdot L(f)_{rad}$. For $V_0 = 1$ V_{RMS} , $L(f) = -190$ dBc/Hz. Since one volt (rms) into 50Ω corresponds to a power level of +13 dBm, $L(f) = -177$ dBc/Hz, referenced to 0 dBm.

Using 0 dBm as the reference level, the room-temperature thermal-noise power relative to the signal power is simply -177 dBm $- (P_{in})$, where P_{in} is the signal power in dBm. The noise figure (NF) is the ratio (in dB units) of excess noise to thermal-noise power and the final formula (in terms of PM noise) is

$$L(f) = -177 + NF - (P_{in}).$$

This is the wideband PM noise floor of an amplifier. The offset frequency f must be high enough to produce the amplifier's characteristic wideband noise level at its output, yet not so high that an

accurate cross-correlation measurement is not obtained, for example, due to system roll-off or operation in an extreme range of the FFT analyzer.

The formula above permits calculation of NF from a $L(f)$ plot by estimating the constant broadband PM noise level and P_{in} . This constant white PM noise is readily apparent only in the fourth measurement (from the top) in figure 6. No white PM level was observed at a power input of -41.6 dBm as shown in the top two plots in figure 6. To reduce the power meter uncertainty when determining P_{in} , we have determined the power at the input to the amplifier inside the dewar by measuring the power at the signal source and then separately measuring the total waveguide attenuation. A valid white PM noise level was observed only at an input power of -51.4 dBm. We assumed that there was no variation in attenuation for the short stainless-steel segment of waveguide in the dewar.

For the cooled InP amplifier, we calculate an average white PM level of -124.8 dBc/Hz for $1 \text{ kHz} < f < 20 \text{ kHz}$. For $f > 100 \text{ kHz}$, this PM noise measurement was subject to spurious broadband pickup of unknown origin, so we have regarded this range as having more uncertainty than the range of 1 kHz to 20 kHz . Based on the incident power to the amplifier, we compute the amplifier's noise figure to be 0.8 dB , which corresponds to a noise temperature of 59 K , or somewhat worse than the 30 K NF measurement made on the best of 17 amplifiers measured by Weinreb, et al.[7]. The 30 K value is in reasonable agreement if we take into account measurement uncertainty.

IX. JITTER CALCULATION

We can estimate the level of the jitter introduced by the InP amplifier at 100 GHz based on the PM measurements here using the tables given in Ref [1] and later refined in Ref [22]. These tables provide an accurate estimate of what would be observed as the clock-signal rms jitter using a conventional oscilloscope or jitter analyzer which measures this characteristic using an "eye" display. An advantage to the technique of transforming PM noise is that there are no trigger errors nor time-base distortions normally associated with an oscilloscope or analyzer[23,24]. Our goal is to find the baseline, or best attainable, performance for those electronic systems using a clock signal as a reference. To be conveniently usable, that reference usually must include the noise of high-performance amplifiers of the type reported here.

To recap, we assume that there exists an ideal, noiseless 100 GHz oscillator that is the source signal for the amplifiers under test. The measurements shown in figure 6 presume this, so it is a matter of mapping the functions from the $L(f)$ domain to jitter(τ), where τ is some sample interval of the 100 GHz oscillating signal. On an oscilloscope or analyzer, τ would be an integer number of periods of clock cycles. From the measurements at $P_{in} = -51.4 \text{ dBm}$, random-walk PM (RWPM) is given by $10^{-6.9}/f^2$ (corresponding, for example, to -109 dBc/Hz at $f = 100 \text{ Hz}$) and white PM (WHPM) is given by $10^{-12.5}$ (-125 dBc/Hz at $f > 1 \text{ kHz}$). We can write a two-function summation of these as

$$L(f) = 10\log(10^{-12.5} + 10^{-6.9}/f^2).$$

At 100 GHz , a 2-period, or two cycle, interval (the shortest interval using tables in Ref's [1] and [22]) corresponds to 20 ps . Therefore, the rms jitter is the sample standard deviation using a mean value obtained from the sample itself of nominally 20 ps . The equivalent oscilloscope for a measurement such as this would be one with a flat frequency response from 50 GHz to 150 GHz when two clock cycles are displayed. The top row of Table 1 displays the results of transforming each of these functions to a 2-period jitter level and obtaining 283 fs , mainly dominated by the WHPM level. At $P_{in} = -41.6 \text{ dBm}$, the 2-period jitter for the InP amplifier is 91.1 fs . We note that FLPM now dominates over the RWPM observed earlier. Above this power input and below saturation, we also find that with a 10 dB increase in P_{in} , there is approximately a 20 dBc/Hz increase in this FLPM noise, while there is a 10 dBc/Hz decrease in WHPM noise. Based on this, the projected jitter for $P_{in} = -31.6 \text{ dBm}$ is 44.2 fs . For comparison, the bottom row is a measurement on the room-temperature

RT amplifier with $P_{in} = -6.4$ dBm and operating a few dB into saturation. Here the FLPM level is actually less as shown in figure 5, and the WHPM level of -150 dBc/Hz is assumed at an offset frequency beyond 10 MHz and was the lowest obtainable level of WHPM in any case. The total computed jitter is 16 fs of the RT amplifier at this input power. Figure 8 plots the jitter based on the levels and types of noise indicated in Table 1.

Table 1: Jitter values for various levels and types of noise. In all cases, the bandwidth is 50GHz and τ is equal to 20 ps, so the last three columns are 2-period jitter values.

P_{in} (dBm)	$L(f)$, WHPM	$L(f)$, RWPM	Jitter(fs), WHPM	Jitter(fs),RWPM	Total Jitter(fs)
-51.4	$10\log(10^{-12.5})$	$10\log(10^{-6.9} / f^2)$	283	5.7×10^{-3}	283
P_{in} (dBm)	$L(f)$, WHPM	$L(f)$, FLPM	Jitter(fs), WHPM	Jitter(fs), FLPM	Total Jitter(fs)
-41.6	$10\log(10^{-13.5})$	$10\log(10^{-6.5} / f)$	89.5	1.59	91.09
-31.6	$10\log(10^{-14.5})$	$10\log(10^{-4.5} / f)$	28.3	15.9	44.2
-6.4	$10\log(10^{-15})$	$10\log(10^{-7.5} / f)$	15.9	0.503	16.003

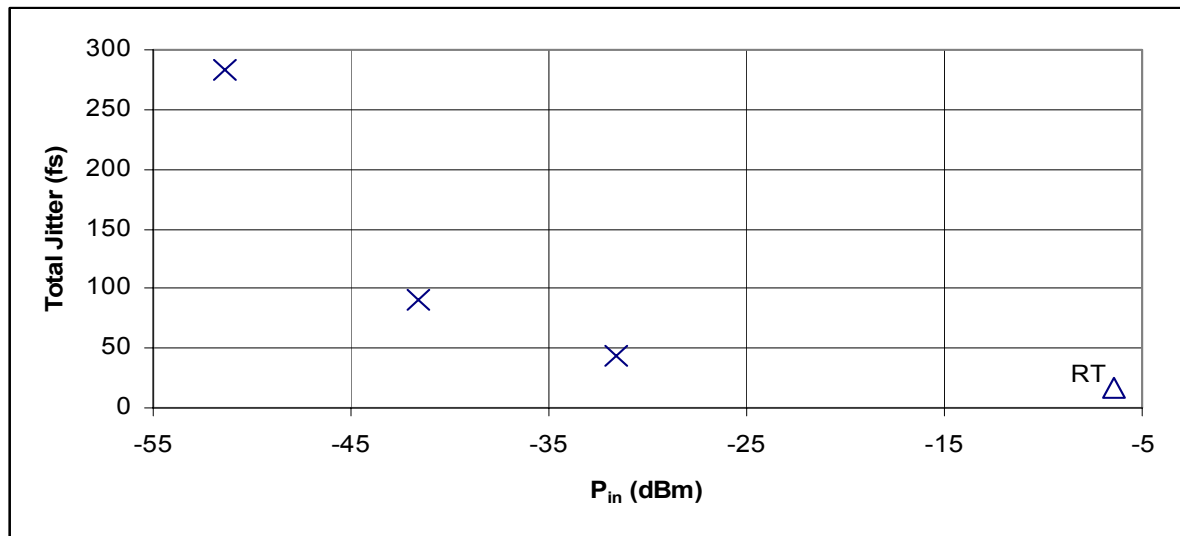


Figure 8: Composite jitter at various input power levels as indicated in Table 1. RT is the room-temperature amplifier.

X. SUMMARY

We have constructed a dual-channel (cross-correlation) noise measurement system and used it to measure the PM and AM noise of 100 GHz InP amplifiers operating at both room temperature and cooled to 77 K. Within measurement uncertainty, there was no notable difference between measurements taken at 5 K and 77 K. At moderate input power, the PM noise of these amplifiers shows f^{-1} , or flicker PM, dependence, and, at the lowest input power, shows f^{-2} , or random-walk PM, dependence. The noise level depends dramatically on the power into the amplifier and has a large effect on the corner frequency at which flicker or random-walk PM noise becomes white PM noise. The corner frequency changed from 1 kHz to >10 MHz for only a 10 dB increase in input power. This indicates significant nonlinearity in the amplifier.

We derived a formula for computing noise figure (NF) from PM noise measurements and used it to estimate NF. The 77 K InP amplifier's NF, based on an input power of -51.4 dBm, was 0.8 dB at using a white PM noise level of -124.8 dBc/Hz. The total NF measurement error is estimated to be ± 0.3 dB.

At cryogenic temperatures, the rms jitter due to the amplifier based on residual PM noise measurements was 44.2 fs in a 20 ps interval at an input power of -31.6 dBm, which operates the amplifier in an unsaturated region. For comparison, jitter obtained from an amplifier operating at room temperature and in saturation was 16 fs in a 20 ps interval with an input power of -6.4 dBm.

XI. ACKNOWLEDGMENTS

We gratefully acknowledge the help of Fred Walls for providing first principles in the derivation of noise figure, and Tiffany Tasset for deriving the values of rms jitter given in Table 1.

References

- [1] D. A. Howe, "Measuring Clock Jitter at 100 GHz from PM Noise Measurements," Proc. of 59th Automatic RF Techniques Group, Microwave Measurements Conference, June 2002.
- [2] E. S. Ferre-Pikal, J. R. Vig, et al., "IEEE 1139-1999: Standard Definitions of Physical Quantities for Fundamental Frequency and Time Metrology--Random Instabilities," Institute of Electrical Engineers, Inc., New York, NY 10017, USA.
- [3] D. B. Sullivan, D. W. Allan, D. A. Howe, and F. L. Walls (Editors), "Characterization of Clocks and Oscillators", National Institute of Standards and Technology Technical Note 1337, Section A-6, March 1990.
- [4] D. W. Allan, H. Hellwig, P. Kartaschoff, J. Vanier, J. Vig, G.M.R. Winkler, and N. Yannoni, "Standard Terminology for Fundamental Frequency and Time Metrology," Proc. of 42nd Annual Symposium and Frequency Control, IEEE Cat. No. 88CH2588-2, 1988, pp. 419-425.
- [5] E. S. Roseblum, "Atmosphere absorption of 10 – 400 KMQS radiation: summary and biography up to 1961," Microwave Journal, vol. 4, pp. 91 – 96, March 1961.
- [6] B. Bhat and S. K. Koul, *Analysis, Design and Applications of Fin Lines*, ch. 1, "Introduction to millimeter-wave circuits," Artech House, Norwood, MA, 1987.
- [7] S. Weinreb, R. Lai, N. Erickson, T. Gaier, and J. Wielgus, "W-band InP Wideband MMIC LNA with 30 K Noise Temperature," Microwave Symposium Digest, 1999 IEEE MTT-S International, vol.1, pp 101-104.
- [8] D. A. Howe, C. Nelson, F. L. Walls, J. F. Nava, A. Hati, and A. Sen Gupta, "A 100 GHz AM and PM Noise Measurement System: Preliminary Design and Performance," Proc. 2002 IEEE International Frequency Control Symposium, May, 2002, pp. 690 - 698.
- [9] D. A. Howe, D. W. Allan, and J. A. Barnes, "Properties of Signal Sources and Measurement Methods," Proc. of 35th Annual Symposium on Frequency Control, 1981, pp. A1-A47; also in NIST Technical Note 1337, March 1990, pp. TN-14-TN-55.
- [10] F. L. Walls, A. J. D. Clements, C. M. Felton, and T. D. Martin, "Accuracy Model for Phase Noise Measurements," Proc. of 21st Annual Precise Time and Time Interval Planning Meeting, Redondo Beach, CA, Nov. 28 - 30, 1989, pp. 295-310.
- [11] F. L. Walls, A. J. D. Clements, C. M. Felton, M. A. Lombardi, and M. D. Vanek, "Extending the Range and Accuracy of Phase Noise Measurements," Proc. of 42nd Annual Symposium on Frequency Control, IEEE Cat. No. 88CH2588-2, 1988, pp. 432-441; also in NIST Technical Note 1337, March 1990, pp. TN-129-TN-137.

- [12] F. L. Walls, A. J. D. Clements, C. M. Felton, and T. D. Martin, "Precision Phase Noise Metrology," Proc. of National Conference of Standards Laboratory (NCSL), 1991 pp. 257-275.
- [13] W. F. Walls, "Cross-Correlation Phase Noise Measurements," Proc. of IEEE Frequency Control Symposium, 1992, pp. 257-261.
- [14] F. L. Walls, C. M. Felton, A. J. D. Clements, and T. D. Martin, "Accuracy Model for Phase Noise Measurements," Proc. 21st Annual Precise Time and Time Interval Planning Meeting, Redondo Beach, CA, pp. 295 – 310, Nov. 30 – Dec. 1, 1990. Details of the calibrator are covered under NIST U. S. Patent No.'s 4,968,908 issued 6 Nov. 1990, "Method and Apparatus for Wide Band Phase Modulation," and 5,101,506 issued 31 Mar. 1992, "Frequency Calibration Standard using a Wide Band Phase Modulator."
- [15] V. P. Koshelets, A. B. Ermakov, et al., "Superfine Resonant Structures on IVC of Long Josephson Junctions and its Influence on Flux Flow Oscillator Linewidth", *IEEE Trans. on Applied Superconductivity*, **11** (No. 1), pp. 1211-124, 2001.
- [16] K. K. Likharev, *Dynamics of Josephson Junctions and Circuits*. Philadelphia, PA: Gordon Breach Science Publishers, 1986, pp. 447-468.
- [17] A. Hati, D. A. Howe, D. Walker, and F. L. Walls, "Noise Figure vs. PM Noise Measurements: A Study at Microwave Frequencies," Proc. 2003 IEEE International Frequency Control Symposium, May, 2003, in process. For preprint: email dhowe@boulder.nist.gov.
- [18] S. Barua, A. M. Van Slyke, and E. S. Ferre-Pikal, "Phase Noise in Heterojunction Field effect Transistor Amplifiers," Proc. 2002 IEEE International Frequency Control Symposium, May, 2002, pp. 710 - 714.
- [19] S. C. Peacock, M. A. Stauffer, A. M. Van Slyke, E. S. Ferre-Pikal, "Study of Flicker Phase Modulation and Amplitude Modulation Noise in Field effect Transistor Amplifiers," Proc. 2001 IEEE International Frequency Control Symposium, June, 2001, pp. 200 - 204.
- [20] S. Galliou, M. Mourey and J. J. Besson, "Comparison of the Effects of Intermodulation and Amplitude to Phase conversion in a Transistor Stage upon the Oscillator Phase Noise," Proc. 1998 IEEE International Frequency Control Symposium, May, 1998, pp. 172 - 177.
- [21] F. L. Walls, E. S. Ferre-Pikal and S. R. Jefferts, "The Origin of 1/f PM and AM Noise in Bipolar Junction Transistor Amplifiers, " Proc. 1995 IEEE International Frequency Control Symposium, May, 1995, pp 294 - 304.
- [22] D. A. Howe and T. N. Tasset, "Clock Jitter Estimation based on PM Noise Measurements," Proc. 2003 IEEE International Frequency Control Symposium, May, 2003, in process. For preprint: email dhowe@boulder.nist.gov.
- [23] G. N. Stenbakken and J. P. Deyst, "Comparison of time base nonlinearity measurement techniques," *IEEE Trans. Instrum. Meas.*, **IM-47**, pp. 34-39, 1998.
- [24] R. Pintelon and J. Schoukens, "An improved sine wave fitting procedure for characterizing data acquisition channels," *IEEE Trans. Instrum. Meas.*, **IM-45**, pp. 588-593, 1996.